

Vladimír Janovský; Petr Procházka  
Contact problem of two elastic bodies. III

*Aplikace matematiky*, Vol. 25 (1980), No. 2, 137–146

Persistent URL: <http://dml.cz/dmlcz/103845>

## Terms of use:

© Institute of Mathematics AS CR, 1980

Institute of Mathematics of the Czech Academy of Sciences provides access to digitized documents strictly for personal use. Each copy of any part of this document must contain these *Terms of use*.



This document has been digitized, optimized for electronic delivery and stamped with digital signature within the project *DML-CZ: The Czech Digital Mathematics Library* <http://dml.cz>

## CONTACT PROBLEM OF TWO ELASTIC BODIES – Part III

VLADIMÍR JANOVSKÝ, PETR PROCHÁZKA

(Received September 1, 1977)

## INTRODUCTION

In Part I and Part II of this paper the problem was formulated and its solution was proposed. Uniqueness and solvability of the original problem were proved and convergence of the finite element solution to the solution of the main problem was established.

In this Part III the implementation of p, A-Algorithm (see Part I) will be presented and a practical analysis of convergence will be shown. While the first and second parts of this paper were written for a mathematician, this part contains mostly remarks concerning practical applications.

The results presented were obtained by programs running on HP 2100 S computer.

## 7. NUMERICAL ANALYSIS

We shall restrict our considerations to the finite element method with linear displacement elements, which has been published in many papers (see [2]). From the above paragraphs we can conclude: The Problems are linear over each of regions  $\Omega'$  and  $\Omega''$ , respectively. The linearity fails along the contact line  $\Gamma$ , where the condition of "continuity" of displacements appears at the artificial bolt  $A$  only, while at the nodal points from the set  $\mathfrak{N}(p) \div A$  the balance condition has to be satisfied.

Implementation of p, A-Algorithm consists of two problems iterated and described as STEP 1 and STEP 2.

If the choice of  $A$  is proper, p-Algorithm and p, A-Algorithm coincide. We choose a point  $A$  considering our choice is a proper one.

STEP 1: Using the terminology of "finite dimensional" elasticity, the relevant problem can be formulated as follows:

For distributed external forces  $\mathbf{g}'$  and  $\mathbf{g}''$  on  $\Omega'$  and  $\Omega''$  (caused by  $F, P$  and the boundary condition on  $\Gamma_s$ ) and distributed contact forces  $\mathbf{f}'$  and  $\mathbf{f}'' = -\mathbf{f}'$  on  $\Gamma$

(caused by  $\lambda^{(p,k)}$  – see STEP 2) given in each iteration step, find the field of displacements  $\mathbf{u}'$  and  $\mathbf{u}''$ , respectively, of the bodies  $\Omega'$  and  $\Omega''$  (2 degrees of freedom at each nodal point) such that the potential energy of  $\Omega'$  and  $\Omega''$ , respectively, is minimal and the geometrical boundary conditions on  $\Gamma_2$ ,  $\Gamma_3$  and  $\Gamma_4$  on  $\mathbf{u}'$  and  $\mathbf{u}''$  are satisfied (restrictions on the corresponding degrees of freedom).\*) Moreover, the side condition has to be satisfied: The normal displacements of  $\mathbf{u}'$  and  $\mathbf{u}''$  at the point  $A$  are continuous (i.e.  $[u]_v = 0$  at  $A$ ).

This problem leads to the solution of two linear algebraic systems given by square stiffness matrices  $\mathbf{K}'$  and  $\mathbf{K}''$ .

$$(7.1) \quad \mathbf{K}'\mathbf{u}' = \mathbf{g}' + \mathbf{f}' ,$$

$$(7.2) \quad \mathbf{K}''\mathbf{u}'' = \mathbf{g}'' + \mathbf{f}'' .$$

The matrix  $\mathbf{K}'$  is regular, while the matrix  $\mathbf{K}''$  is singular, i.e. the system (7.2) is solvable for “suitable” right hand sides only and a solution  $\mathbf{u}''$  (if it exists) is not unique. Nevertheless, it can be shown that  $\mathbf{g}'' + \mathbf{f}''$  is always “suitable” if  $\mathbf{f}''$  is a distributed force given by  $\lambda^{(p,k)}$ , where  $\lambda^{(p,k)}$  solves STEP 2 (because of balance condition, see Remark 3.4) and  $\mathbf{u}''$  is uniquely determined up to a rigid displacement in the  $x_2$ -direction.

The general strategy of solving STEP 1:

- (A) solve (7.1);
- (B) find the particular solution  ${}^-\mathbf{u}''$  to the system (7.2) using the condition that there is no  $v$ -displacement at  $A$  (then  ${}^-\mathbf{u}''$  is uniquely determined – the body  $\Omega''$  is statically determined);
- (C) make the superposition of  ${}^-\mathbf{u}''$  and a rigid admissible displacement  $\sim\mathbf{u}''$  of  $\Omega''$  in the  $x_2$ -direction, i.e. set

$$(7.3) \quad \mathbf{u}'' = {}^-\mathbf{u}'' + \sim\mathbf{u}''$$

so that  $\mathbf{u}''$  satisfies the side condition  $[u]_v = 0$  at  $A$ .

The way of finding  $\sim\mathbf{u}''$  becomes clear from Fig. 10, where  $A'$  and  $\bar{A}''$  are the positions of  $A$  after the deformation of  $\Omega'$  and  $\Omega''$  via (A) and (B) and  $A''$  is the position of  $A$  after the superposition (7.3). The point  $A''$  exists uniquely by virtue of the assumption that  $A \in N_0^{(p)}$ , i.e. the  $v$ -direction is not perpendicular to the  $x_2$ -axis.

The direction of the outward normal to  $\Omega'$  at a nodal point  $N_{i,p}$  will be chosen as the axis of the angle which is defined by points  $N_{i-1,p}$ ,  $N_{i+1,p}$ , for  $i = 1, \dots, k(p) - 1$ . For nodal points belonging to the  $x_2$ -axis the outward normal has the direction of the positive or the negative  $x_2$ -axis. With respect to small deformation theory, this is a sufficiently suitable choice.

We remark that from the algebraic point of view the step (B) consists in replacing one of the equations (7.2), which are linearly dependent, by the condition “no

\*) We omit indices  $p, k$ .

$v$ -displacement at  $A''$ . We now briefly explain which equation from (7.2) has to be replaced:

Each equation of (7.2) is “connected” with one degree of freedom of the body  $\Omega''$  and expresses the condition of the minimal energy, assuming that all degrees of freedom are “frozen” except the relevant one. It can be shown that the equation “connected” with the  $v$ -displacement at the point  $A$  (after geometrical transformation) is redundant and has to be replaced by the condition “no  $v$ -displacement at  $A''$ ”.

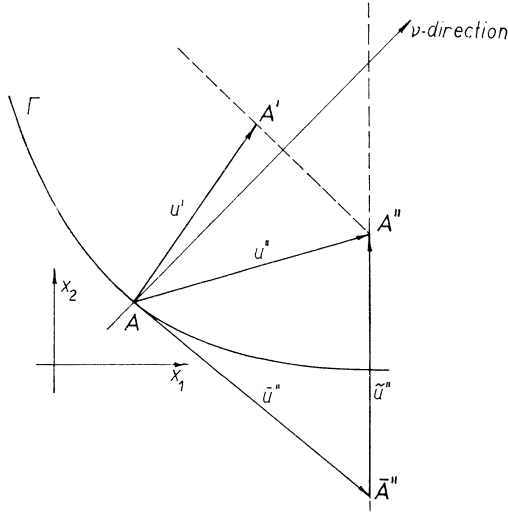


Fig. 10.

The great advantage is the splitting of  $\mathbf{u}'$  and  ${}^{-}\mathbf{u}''$ :

$$(7.5) \quad \mathbf{u}' = \mathbf{u}'_g + \mathbf{u}'_f, \quad {}^{-}\mathbf{u}'' = {}^{-}\mathbf{u}''_g + {}^{-}\mathbf{u}''_f$$

where  $\mathbf{u}'_g, \mathbf{u}'_f, {}^{-}\mathbf{u}''_g, {}^{-}\mathbf{u}''_f$  solve linear algebraic systems

$$(7.6) \quad \mathbf{K}'\mathbf{u}'_g = \mathbf{g}', \quad {}^{-}\mathbf{K}''\,{}^{-}\mathbf{u}''_g = \mathbf{g}''$$

and

$$(7.7) \quad \mathbf{K}'\mathbf{u}'_f = \mathbf{f}', \quad {}^{-}\mathbf{K}''\,{}^{-}\mathbf{u}''_f = \mathbf{f}''$$

where  ${}^{-}\mathbf{K}''$  is the matrix  $\mathbf{K}''$  adapted with respect to the condition “no  $v$ -displacement” at  $A$ . The linearity admits the superposition of the influence of the forces  $\mathbf{f}$  and  $\mathbf{g}$ , i.e.  $\mathbf{u}'_g$  and  ${}^{-}\mathbf{u}''_g$  can be computed once only and they do not change during iterations between STEP 1 and STEP 2.

We briefly explain how to compute the values of vectors  $\mathbf{u}'_g$  and  ${}^{-}\mathbf{u}''_g$ . At the beginning of iteration we fix the point  $A$  at the place before deformation and solving

the second equation (7.6) we obtain the solution  ${}^{-}\mathbf{u}_g''$  and the normal reaction at  $A$ . This reaction can be obtained either numerically or from the balance condition in the  $x_2$ -axis direction. Denote the reaction by  $R_A$ . Then do the same with the first equation (7.6) with a free (non-fixed point)  $A$ , considering  $R_A$  as a known external force at the nodal point  $A$  with respect to  $\Omega'$ . We obtain the solution  $\mathbf{u}_g'$ .

To “feed” STEP 2 and hence to repeat the algorithm, we are actually interested in the values of  $\mathbf{u}'$  and  $\mathbf{u}''$  on  $\Gamma$ . Even, we have only to compute  $\mathbf{u}_f'$  and  ${}^{-}\mathbf{u}_f''$  on  $\Gamma$ . From this point of view we recommend the pre-elimination (condensation of parameters) of both the matrices  $\mathbf{K}'$  and  ${}^{-}\mathbf{K}''$ , using Gaussian elimination in the following sense: We transform  $\mathbf{K}'$  as well as  ${}^{-}\mathbf{K}''$  to the form

$$\begin{bmatrix} \mathbf{A}_{11} & \mathbf{A}_{12} \\ 0 & \mathbf{A}_{22} \end{bmatrix}$$

considering the renumbering of the nodal points as follows: The nodal points on the contact line  $\Gamma$  have the numbers  $K'(p) - k(p) + 1, \dots, K'(p)$  with respect to  $\Omega'$  and  $K''(p) - k(p) + 1, \dots, K''(p)$  with respect to  $\Omega''$ , where  $K'(p)$  and  $K''(p)$  are the numbers of nodal points of triangulations of  $\Omega'$  and  $\Omega''$ , respectively. This means that the last numbers of the numbering belong to the nodal points on the contact line  $\Gamma$ . The matrix  $\mathbf{A}_{22}$  has the dimension  $(2k(p) \times 2k(p))$  i.e. it is a square matrix and  $\mathbf{A}_{11}$  has zeros under the pivots and remains banded. The relevant values  $\mathbf{U}_f'$  and  ${}^{-}\mathbf{U}_f''$  of  $\mathbf{u}_f'$  and  ${}^{-}\mathbf{u}_f''$  on  $\Gamma$  are given by “small” linear algebraic systems

$$(7.8) \quad \mathbf{K}'\mathbf{U}_f' = \mathbf{F}', \quad {}^{-}\mathbf{K}''{}^{-}\mathbf{U}_f'' = \mathbf{F}''.$$

The size of the regular square matrices  $\mathbf{K}'$  and  $\mathbf{K}''$  is now  $2k(p) \times 2k(p)$  and this elimination proceeds in such a way that we do not change the right hand sides of equations (7.7), i.e. the mappings

$$(7.9) \quad \mathbf{f}' \rightarrow \mathbf{F}', \quad {}^{-}\mathbf{f}'' \rightarrow {}^{-}\mathbf{F}''$$

are just restrictions.

Resume of STEP 1.

The input to STEP 1 is  $\lambda$ . The output is  $[u]_v$  at nodal points on  $\Gamma$ . The actual computation consists of

- (1) computation of  $f'$  (i.e. substitution in simple formulae),
- (2) solution of two “small” linear systems (7.8),
- (3) evolution of (7.5) on  $\Gamma$ ,
- (4) finding of the shift  $\tilde{u}''$  at  $A$  – via Fig. 10,
- (5) superposition (7.3) on  $\Gamma$ ,
- (6) calculation of  $[u]_v$  on  $\Gamma$ .

Hence the matrix inversion, which is the most time consuming operation, is reduced to two matrices having size  $2k(p) \times 2k(p)$ . It is seen that p, A-Algorithm is extra-

ordinarily advantageous when the relative number of nodal points on the contact line is small.

STEP 2: There is only one difficulty in the computation of  $\lambda^{(p,k+1)}$ . This concerns the choice of the parameter  $\varrho$ , which can dramatically influence the convergence of p, A-Algorithm. From the theoretical point of view, this algorithm can be regarded as a method for finding a fixed-point to an operator on the set  $V_A^{(p)} + A_A^{(p)}$ .

In the proof of Theorem 3.4 (see [3]) the “convergent” choice was theoretically guaranteed, namely the interval (3.15) is an optimal choice of  $\varrho$  in a certain sense. Anyway, the interval (3.15) is not necessarily available in practice, as was said in Remark 3.5. We have carried out a lot of computations and Fig. 11 reflects our experience concerning the choice of  $\varrho$  in our particular problem. Fig. 11 shows the typical dependence of the number of iterations needed to reach a given precision on the value of  $\varrho$ .

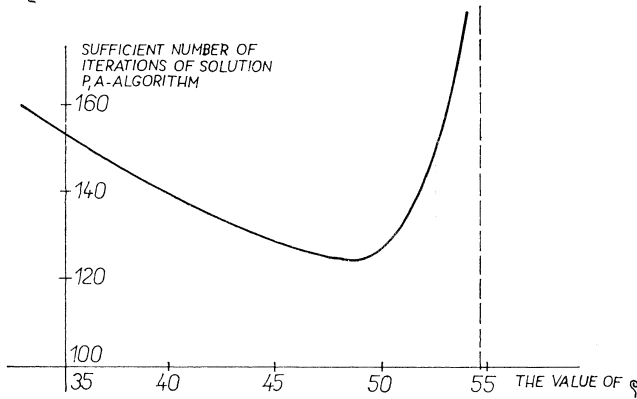


Fig. 11.

## 8. RESULTS

To check the accuracy and to determine the rate of convergence with respect to the number of elements employed (in particular with respect to the number of nodal points on the contact line) two problems with the same physical properties were analysed. To our great regret we cannot compare our results with some practical model because none is available to us.

The general geometry of our model example is illustrated in Fig. 12. A plate with sides  $40\text{ m} \times 80\text{ m}$  and a circular contact line with the radius of  $15\text{ m}$  and the tunnel wall of thickness equal to  $3\text{ m}$  were symmetric with respect to both  $x_1$  and  $x_2$  axes. The following physical properties are considered:  $E_{\Omega'} = 2000\text{ Mp/m}^2$ ,  $E_{\Omega''} = 2100000\text{ Mp/m}^2$ ,  $\nu_{\Omega'} = 0.25$  and  $\nu_{\Omega''} = 0.15$ .

The construction was subjected along the line  $\Gamma_1$  to the uniformly distributed load  $q = 50\text{ Mp/m}$ . Along the parts of boundary  $\Gamma_2$ ,  $\Gamma_3$  and  $\Gamma_4$ , there are no displace-

ments in normal direction in the first case. In the second case the vertical part of  $\Gamma_2$  is considered as a free edge, that means it is not prevented from moving.

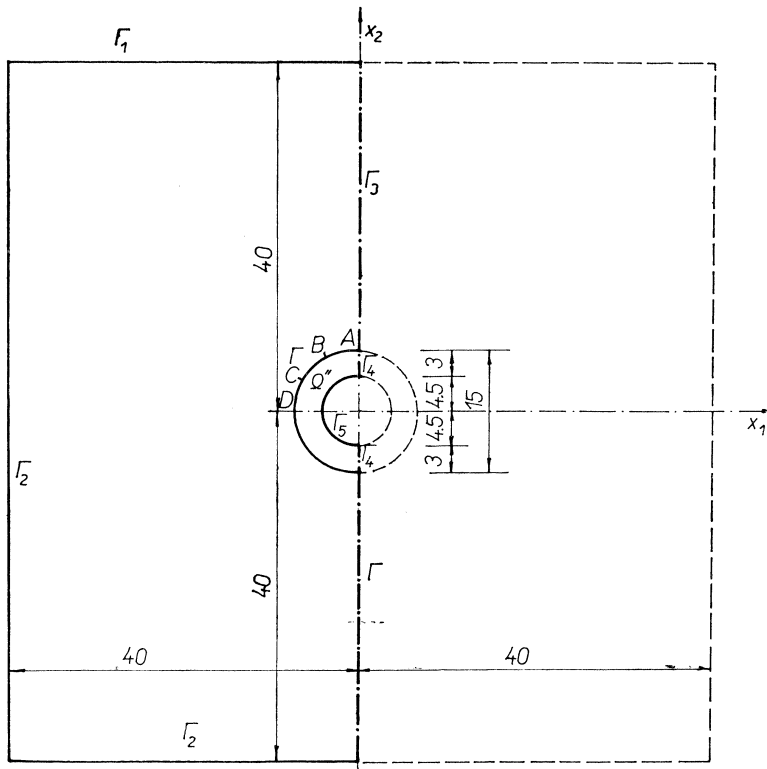


Fig. 12.

The mesh was automatically generated and was refined in the direction from point A to D (see Figs. 12 and 13). The mesh sizes used for computation are as follows: The first model contains 15 nodal points on the contact line, the second 31 and finally, the third model contains 39 nodal points on the contact line. The model with the finest division contains 1404 elements and 759 nodal points. The other models are divided proportionally to the number of nodes on  $\Gamma$ . The results corresponding to the mentioned models are given in Tables. Together with the results for displacements and forces evaluated in normal direction to the contact line the percentage errors are given in Tables. The percentage errors are calculated as

$$\frac{\text{solution of model} - \text{solution on finest mesh}}{\text{solution on finest mesh}} 100\%$$

so that an overestimation will be shown by a positive sign and an underestimation by a negative sign. The finest mesh is that with 39 nodal points on the contact line.

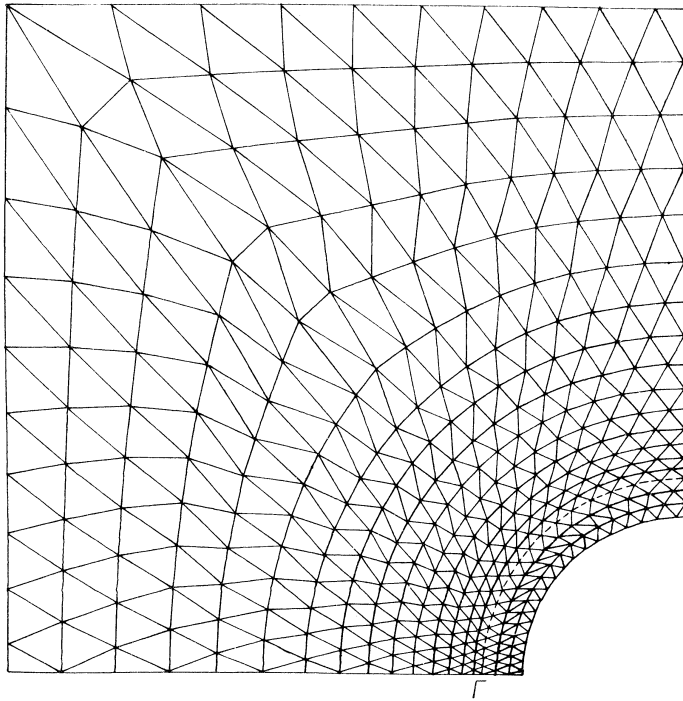


Fig. 13.

Because of the symmetry of the construction about the  $x_1$ -axis, only the upper part of the finest mesh is illustrated in Fig. 13. The refinement in the neighbourhood of the point D (according to the notation in Fig. 12) is obvious from Fig. 13. The situation of the points A, B, C and D at which the values are given is described in Fig. 12. The values at B and C are calculated as the arithmetic mean of the values obtained at the adjacent nodal points.

Tables contain the results obtained for the first and second case of the supporting of the plate studied. The second case of supporting induces a dislocation on the contact line so that the displacements of the earth medium and the displacements of the wall of the tunnel ( $\Omega''$ ) are different along a certain line of the contact line. The normal forces are equal to zero over that part of  $\Gamma$ .

In both cases the results are compared with the results given by the model containing 39 nodal points on the contact line. The finest mesh solution is shown in the last column of Tables.

TABLES

1. model case					
Nodal point on $\Gamma$ -line	displacements on $\Gamma$ -line				
	15-approx	% error	31-approx	% error	39-approx
A	-0.0548	-46.80	-0.0983	-4.56	-0.1030
B	-0.0206	-56.08	-0.0452	-3.62	-0.0469
C	0.0389	-35.38	0.0580	-3.65	0.0602
D	0.0662	-43.52	0.1099	-6.23	0.1172
Nodal point on $\Gamma$ -line	normal forces on $\Gamma$ -line				
	15-approx	% error	31-approx	% error	39-approx
A	0.1675	-14.89	0.1838	-6.61	0.1968
B	0.5883	0.68	0.5782	-1.04	0.5843
C	1.4048	2.42	1.3721	0.00	1.3716
D	1.6263	-2.80	1.6678	-0.32	1.6732
2. model case					
Nodal point on $\Gamma$ -line	displacements with respect to earth				
	15-approx	% error	31-approx	% error	39-approx
A	-6.3954	- 5.30	-6.6487	-1.55	-6.7534
B	-1.5050	3.45	-1.5579	7.09	-1.4548
C	0.0437	-44.54	0.0763	-3.30	0.0788
D	0.0871	-44.20	0.1424	-8.75	0.1561
Nodal point on $\Gamma$ -line	displacements with respect to wall				
	15-approx	% error	31-approx	% error	39-approx
A	-0.0769	-46.45	-0.1357	-5.51	-0.1436
B	-0.0320	-53.62	-0.0687	-0.43	-0.0690
C	0.0437	-44.54	0.0762	-3.30	0.0788
D	0.0871	-44.20	0.1424	-8.75	0.1561
Nodal point on $\Gamma$ -line	normal forces on $\Gamma$ -line				
	15-approx	% error	31-approx	% error	39-approx
A	0.0000		0.0000		0.0000
B	0.0000		0.0000		0.0000
C	1.3941	2.93	1.3535	-0.07	1.3544
D	1.8074	-3.99	1.8713	-0.60	1.8826

We can obviously deduce from Tables that at most of points belonging to the contact line the convergence is monotone. But, in some cases an enormously high error can occur. This is caused by circumstances, mainly by a choice of nodal points along the contact line.

Anyway, the convergence of nodal forces is much better than that of displacements. Even in the case of approximation with 15 nodal points on contact line we obtain sufficient agreement with the results of approximation with 39 nodal points on  $\Gamma$ .

The practical implementation of the presented algorithm confirmed that it is very efficient if the relaxation parameter  $\varrho$  is chosen in an "optimal way". Yet we have to rely more or less on our guess and experience. This lack of information might be improved in the future.

## CONCLUSION

In this paper a contact problem of two elastic bodies has been investigated on an example of a tunnel wall surrounded by earth. The problem is formulated in terms of the constrained minimization of a potential energy functional in the first part [3] where also the solvability and uniqueness are proved and a finite element algorithm based on Uzawa's algorithm is proposed and discussed.

In the second part [4], convergence of the numerical solution to the solution of the original problem has been proved.

In the third part, convergence of the algorithm is investigated on some practical model examples and the practical implementation of the algorithm is discussed.

We remark that in technical practice the model example described in the previous chapters could be generalized for more complicated geometry and mechanical parameters. In DP-Metroprojekt, Prague, a problem concerning the coefficient of Coulomb not equal to zero was examined.

**Acknowledgement.** Thanks are due to Professor J. Nečas and I. Hlaváček for helpful suggestions.

## References

- [1] *J. Céa*: Optimisation théorie et algorithmes. Dunod, Paris 1971.
- [2] *O. C. Zienkiewicz*: The finite element method in engineering science. Mc Graw-Hill, London 1971.
- [3] *V. Janovský, P. Procházka*: Contact problem of two elastic bodies — Part I. *Apl. mat.* 25 (1980), 87—109.
- [4] *V. Janovský, P. Procházka*: Contact problem of two elastic bodies — Part II. *Apl. mat.* 25 (1980), 110—130.

## Souhrn

### KONTAKTNÍ PROBLÉM DVOU PRUŽNÝCH TĚLES

VLADIMÍR JANOVSKÝ, PETR PROCHÁZKA

V této práci je studován kontaktní problém dvou pružných těles s možnou aplikací na výpočet deformace a napjatosti horninového kontinua, oslabeného tunelem s obezdívkou. V první části práce [3] je podána variační formulace problému, navržen konečně-dimenzionální model a jeho řešení na bázi konečných prvků. Ve druhé části [4] je dokázána konvergence numerického řešení k řešení výchozí úlohy. Konečně třetí část práce je věnována praktickému užití navrženého algoritmu a je sledována konvergence na dvou příkladech s ohledem na zhušťující se síť konečných prvků.

*Authors' addresses:* Dr. *Vladimír Janovský*, CSc., MFF KU, Malostranské nám. 25, 118 00 Praha 1, Dr. Ing. *Petr Procházka*, CSc., PÚ VHMP, Žitná 49, 110 00 Praha 1.